NOAA Technical Memorandum ERL WPL-107

OPTIMIZATION FOR THE ALGORITHMS OF AN OPERATIONAL LASER WEATHER IDENTIFIER

Ting-i Wang
D. C. Brinning
G. R. Ochs
R. S. Lawrence

Wave Propagation Laboratory
Boulder, Colorado
October 1982

noaa NATIONAL OCEANIC AND ATMOSPHERIC ADMINISTRATION / Environmental Research Laboratories

NOAA Technical Memorandum ERL WPL-107

OPTIMIZATION FOR THE ALGORITHMS OF AN OPERATIONAL LASER WEATHER IDENTIFIER

Ting-i Wang
D. C. Brinning
G. R. Ochs
R. S. Lawrence

Wave Propagation Laboratory
Boulder, Colorado
October 1982

UNITED STATES
DEPARTMENT OF COMMERCE
Malcolm Baldrige,
Secretary

NATIONAL OCEANIC AND
ATMOSPHERIC ADMINISTRATION
John V. Byrne,
Administrator

Environmental Research
Laboratories
George H. Ludwig
Director

CONTENTS

ABSTRACT. 1

1. INTRODUCTION 1

2. INSTRUMENTATION 3

3. OPTIMIZATION OF THE VERTICAL SPACING 9

4. PRECIPITATION IDENTIFICATION 10

5. SNOW, RAIN, AND HAIL DISCRIMINATION 15

6. DISCUSSIONS 21

REFERENCES 24-25

OPTIMIZATION FOR THE ALGORITHMS OF AN OPERATIONAL LASER WEATHER IDENTIFIER

Ting-i Wang, D.C. Brinning, G.R. Ochs, and R.S. Lawrence
NOAA/ERL/Wave Propagation Laboratory
Boulder, Colorado 80303

ABSTRACT

We have built a prototype Laser Weather Identifier (LWI) including the vertical velocity measurement. The instrument has been collecting data since March 1981 for various types of precipitation. In this report, we discuss the data analysis and give our recommendations for the algorithms of an operational LWI.

1. INTRODUCTION

An early version of the Laser Weather Identifier (LWI) derives its information only from a spectrum analysis. The performance of the system for identifying rain is excellent. It has never missed any rain rates greater than 0.25 mm/h. The system has identified rain traces as much as three hours before the first tip of the tipping-bucket rain gauge. For extremely light rain (no recorded amount of water), the system indicates a 15 percent error rate compared with the human observer's record (Wang et al., 1980). However, it should be pointed out that the weather identifiers were located 1.5 km from the observer, so the spatial variation of precipitation may have contributed to that discrepancy. Also, no attempt was made to estimate and correct for human observer errors.

Because the spectrum of the snow-induced scintillation is close to that of turbulence-induced scintillation (especially during strong

wind), occasional ambiguity occurs. We found it is less accurate to identify snow than rain without introducing more information. The use of spectra alone is insufficient to separate hail from rain because of the similarity in the temporal spectra of their induced scintillations.

Several years ago, we developed a technique for using optical scintillations to measure path-averaged terminal velocity distributions of falling precipitants (Earnshaw et al., 1978; Wang et al., 1979). The general approach is to measure the precipitation induced irradiance scintillations with two horizontally oriented, vertically spaced, line detectors. The temporal covariance function of the signals detected by the two sensors yields the path-averaged terminal velocity distribution of the precipitants. The measured vertical velocity can be used to identify rain, snow, and hail (Earnshaw et al., 1978). An estimated improvement of the error rates with the velocity measurements is shown in Table I.

Table I.--Estimated error rates with and without the vertical velocity measurements for precipitation identifications

Weather / Techniques	Snow	Rain	Hail
Spectra only	30% (Turbulence contamination)	20%	100% (Cannot be separated from rain)
Spectra and vertical velocity	Less than 10%	Less than 10%	Less than 10%

A recent study (Wang, 1981) has shown that the correlation technique can be used in the near-field region as well as in the far-field region of precipitants. This enables us to use the scintillation correlation technique to measure terminal velocity distributions for pathlengths from a few centimeters to a few hundred meters.

Quantitative measurement of total water content for precipitation is also possible (Wang et al., 1978, 1979). Although the technique was developed to measure path-averaged rain rates, it gives a reasonable estimate for total water content for both snow and hail. An estimated accuracy for each type of precipitation is shown in Table II. In addition, if rain is positively identified, the raindrop size-distribution can be obtained (Wang et al., 1979).

Table II.--Estimated accuracy of quantitative measurement of total water content for precipitation

	Snow	Rain	Hail
Accuracy	Order of magnitude	10%	Within a factor of 2

In this report, we discuss the performance of a prototype operational LWI with the vertical velocity measurements. We also give our recommendations for the algorithms of the modified system.

2. INSTRUMENTATION

A prototype operational LWI with the vertical velocity measurements was designed and built by the Wave Propagation Laboratory in Boulder, Colorado. A schematic diagram of the instrument is shown in Fig. 1. The transmitter contains a 4-mw CW He-Ne laser. A divergent lens in front of the laser expands the beam to form a 110 mw uniform beam. The receiving optical system consists of a narrow slitted mask, a converging lens, a field-stop mask at the focal plane of the lens, and a photodetector. Two 1- x 110-mm horizontal slits were used on the mask in front of the lens for irradiance scintillation measurements. The vertical separation between the two slits can be varied from 15- to 30-mm.

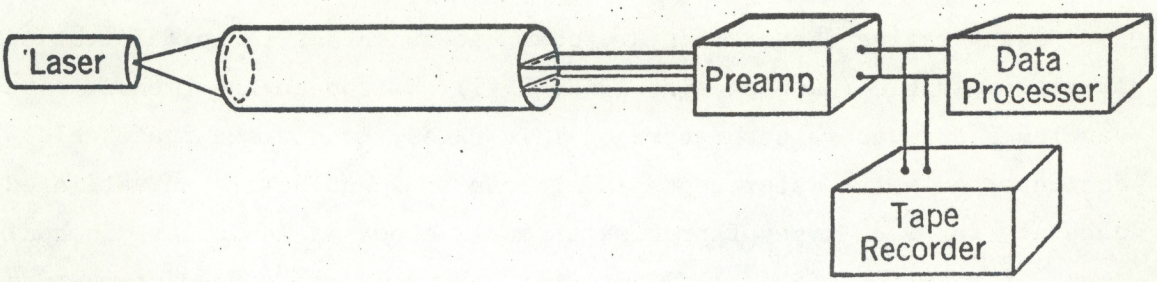

Fig. 1. A schematic diagram of a prototype Laser Weather Identifier.

The signals from the two photodetectors are fed into two separate but identical electronic channels. To reduce the effect of small changes in laser output or beam position, we used a logarithmic amplifier as a normalizer. The input irradiance can be decomposed into a fluctuating part I_1, and an unperturbed part I_o. The photodetector converts to voltages V_1 and V_o respectively. When the voltages are passed through a log-amplifier, the output is

$$\ell n(V_o + V_1) = \ell n\, V_o + \ell n(1 + \frac{V_1}{V_o}) \quad . \tag{1}$$

After transmission through a high pass filter, the final output is $\ell n(1 + V_1/V_o)$. Under ordinary conditions $V_1 << V_o$, and

$$\ell n(1 + \frac{V_1}{V_o}) \simeq \frac{V_1}{V_o} \quad . \tag{2}$$

Therefore the final output is the fractional fluctuations, independent of the absolute irradiance.

The output of the log-amplifier is fed through a low pass filter (cutoff frequency = 5.3 kHz) and a high pass filter (cutoff frequency = 15 Hz). In the ordinary condition, the output is a few tenths of a volt and suitable for tape recording. The gain of the log-amplifers was

1 V/decade. The total gain G of the combination of the high-pass filter, low-pass filter, and the buffer amplifier is 11.9, hence the final output voltage E_o is

$$E_o = 27.5 \frac{V_1}{V_o} \quad . \tag{3}$$

A detailed description of the transmitter, the receiver, and the preamplifier appears in an earlier report (Wang et al., 1982).

To preserve flexibility in the data processing, we recorded the two output signals of the preamplifier on a commercial audio stereo reel-to-reel tape recorder. Because we were interested in frequency components lower than 4 kHz, we used the slowest taping speed (4.75 cm/s) to record more than six hours of data on a single side of a 1100-m (3600-ft) tape. The recorded tapes can then be played back anytime for data analysis. To play back the tape at the fastest speed (19 cm/s) of the tape recorder has many advantages. It speeds up the data processing time by a factor of four. It extends the time constant of the data processor from 22 s to 88 s, the latter was found necessary to suppress the random fluctuations of extremely low precipitation induced signals. To obtain a reliable correlation curve, we found that the low cutoff frequency of the system should be 20 Hz or lower. By recording the data at 4.75 cm/s and playing back at 19 cm/s, we were able to extend the tape recorder cutoff frequency to less than 15 Hz (see Fig. 2). Although the frequency response was not flat, it is good enough for our purpose. For comparison, we also plotted the frequency response of recording and playing back speed at 19 cm/s. Even in this highest speed, the low cutoff frequency was an octave too high.

A schematic diagram of the data processor is shown in Fig. 3. The input can be either from the preamplifier output or from a tape recorder playing back the prerecorded tapes. A time-lagged correlator (Ochs et al., 1981) calculates the subtracted temporal cross-correlation $C_s(\tau)$ of the two input signals namely A(t) and B(t) (Wang et al., 1982), i.e.,

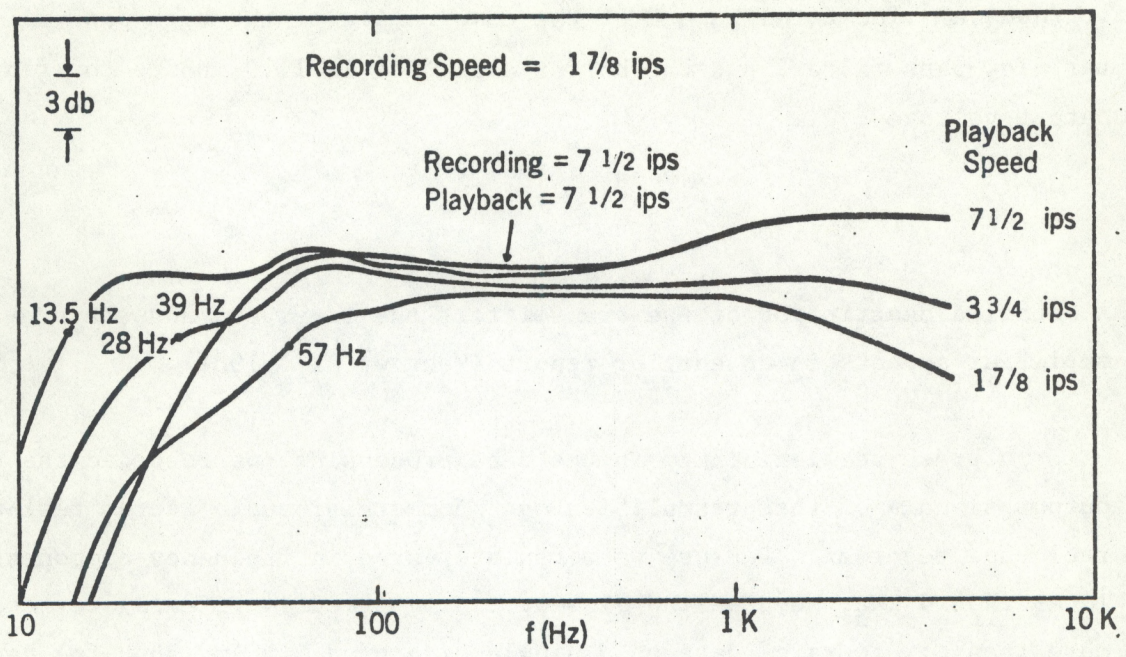

Fig. 2. Tape recorder frequency response for three playback speeds (7 1/2, 3 3/4, and 1 7/8 ips). The recording speed is 1 7/8 ips. The frequency response of recording and playback speeds, both at 7 1/2 ips, are shown for comparison.

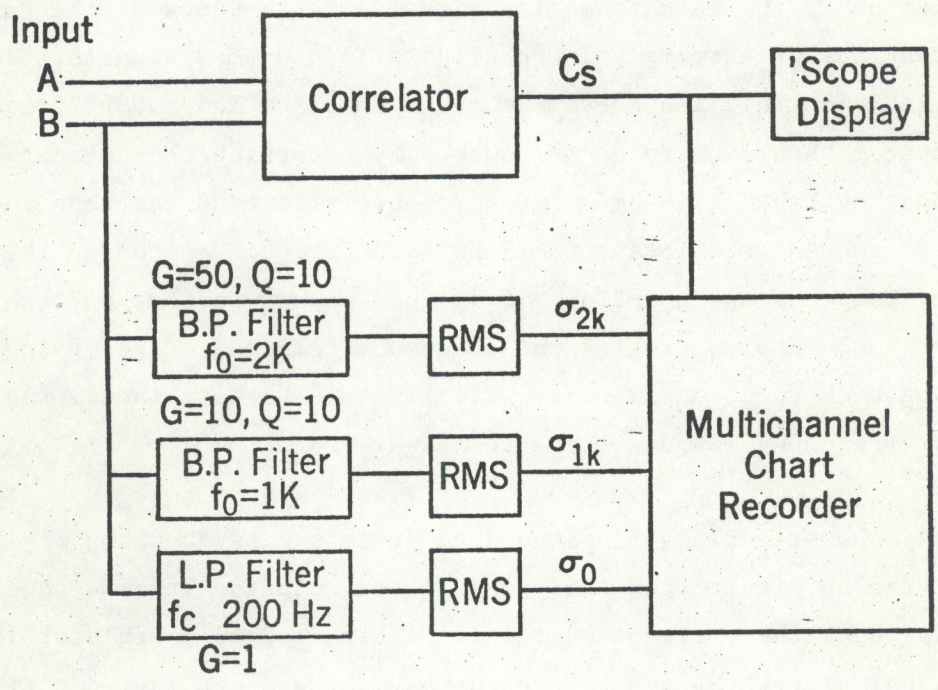

Fig. 4. A schematic diagram of the data processor.

$$C_s(\tau) = \langle A(t)\ B(t+\tau)\rangle_t - \langle A(t+\tau)\ B(t)\rangle_t \ , \qquad (4)$$

where $\langle\ \rangle_t$ denotes the average over a time period. The output of the correlator can be displayed on either an oscilloscope (15 kHz sampling frequency) or a chart recorder (5 Hz sampling frequency).

One of the input signals was also put through narrow bandpass filters and rms measurements for spectral analysis (Fig. 3). The rms value was measured for signal frequencies between 20 Hz and 200 Hz (σ_o), for signal frequencies around 1 kHz (σ_{1k}), and for signal frequencies around 2 kHz (σ_{2k}). The response curves of all three filters are shown in Fig. 4. A detailed circuit diagram is shown in Fig. 5. Four outputs were

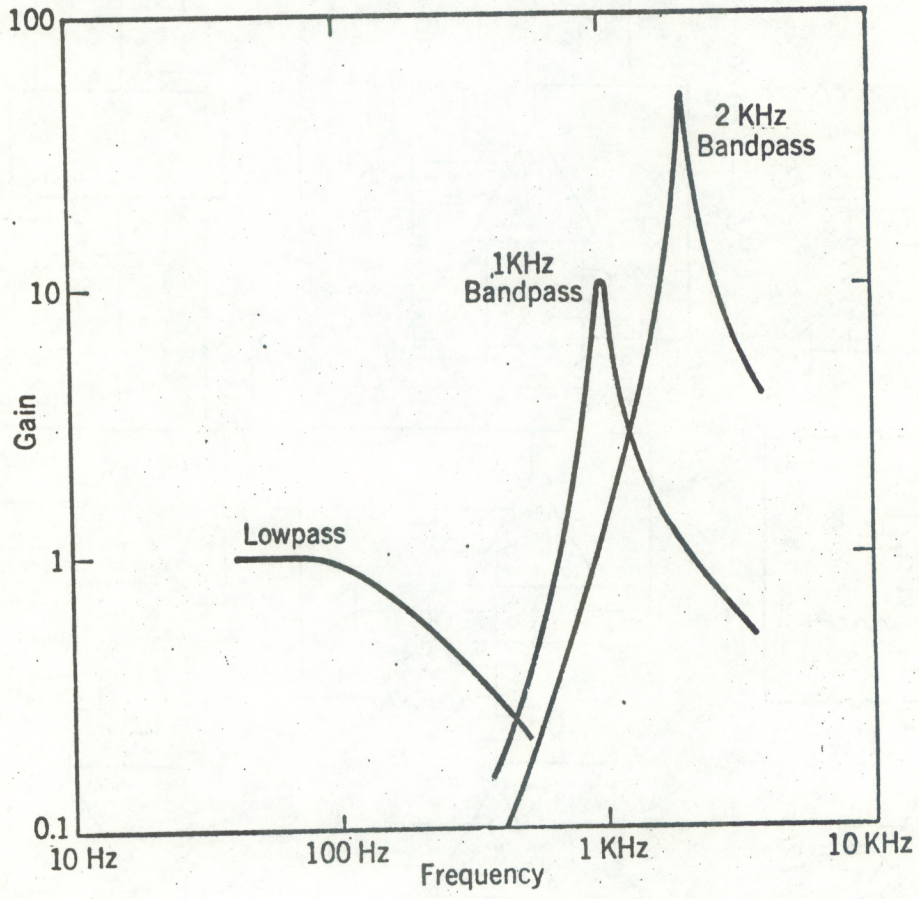

Fig. 4. The frequency response curves of the three filters used in the data processor.

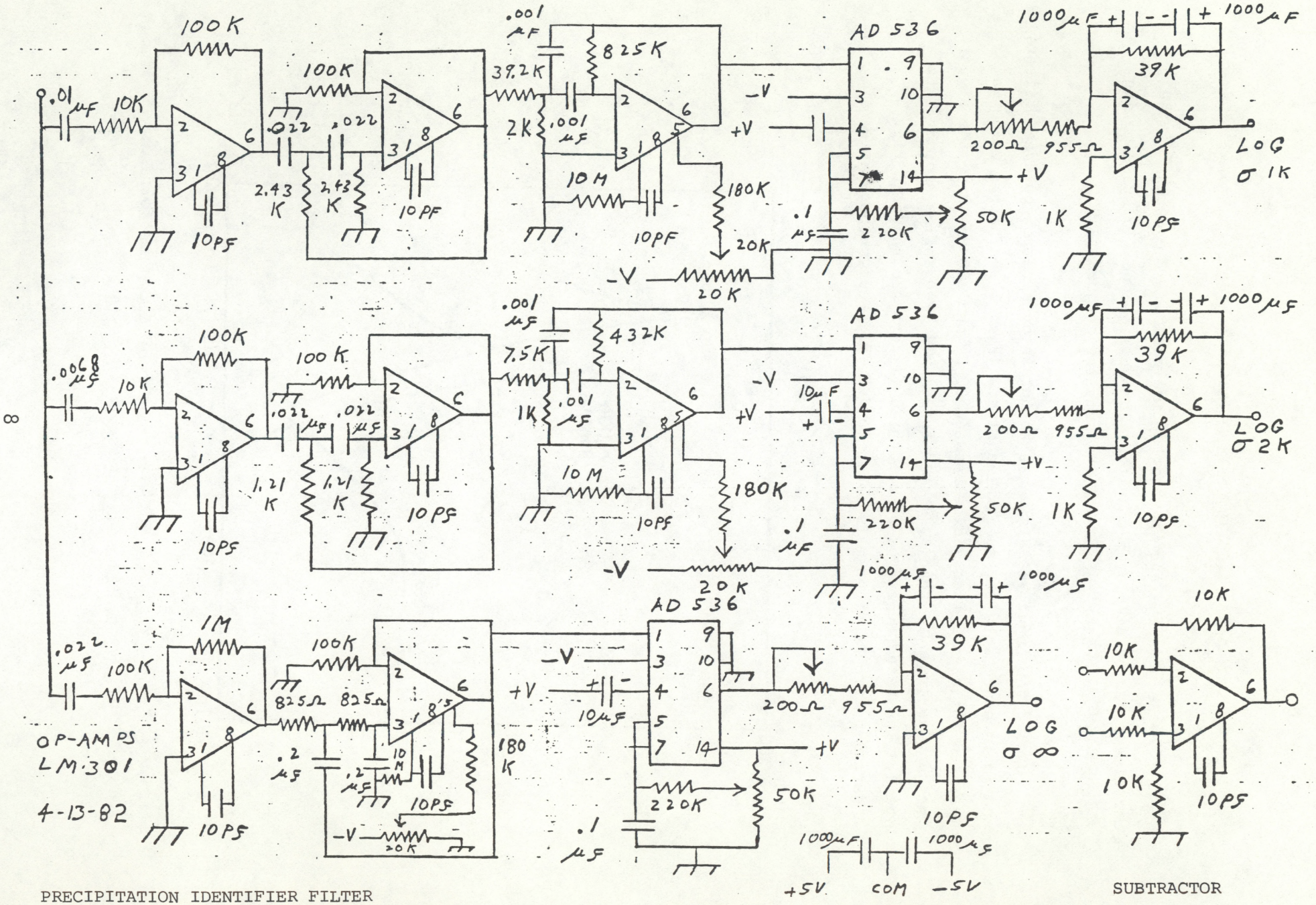

Fig. 5. The circuit diagram of the data processor.

used; i.e., $\log(\sigma_{1k}/\sigma_o)$, $\log(\sigma_{2k}/\sigma_o)$, and $\log(\sigma_{2k}/\sigma_{1k})$. Either $\log(\sigma_{1k}/\sigma_o)$ or $\log(\sigma_{2k}/\sigma_o)$ may be used to identify the precipitation, $\log(\sigma_{1k})$ may be able to give the precipitation rates, and $\log(\sigma_{2k}/\sigma_{1k})$ may be used to discriminate rain and snow (Wang et al., 1981). Using various combinations of spectral and correlation analyses, we can optimize the algorithms of the LWI.

3. OPTIMIZATION OF THE VERTICAL SPACING

The time-lagged cross-correlation function of the amplitude scintillation of two line detectors with length ℓ and vertical separation z_o is (Wang and Lawrence, 1977)

$$C_\chi(z_o, \tau) \sim \frac{z_o^2}{\ell\, \tau^3} \overline{p(a')} \ , \tag{5}$$

where $\overline{p(a')}$ is the path-averaged probability-density function of precipitation particle size, and (in SI units)

$$a' = 2.5 \times 10^{-5}\, z_o^{\,2}\, \tau^{-2} \ . \tag{6}$$

We assume that $\overline{p(a')}$ follows an exponential distribution (the Marshall-Palmer distribution is a special case of the exponential distribution), i.e.,

$$\overline{p(a')} \sim \exp(-2\Lambda\, a')$$

$$= \exp(-5 \times 10^{-5}\, \Lambda\, z_o^{\,2}\, \tau^{-2}) \ , \tag{7}$$

where Λ is a parameter inversely proportional to the mean size. Inserting Eq. (7) into Eq. (5) and finding the maximum of C_χ, we obtain

$$C_\chi(z_o, \tau_p) \sim z_o^{-1} \ , \tag{8}$$

where $\tau_p = 3.16 \times 10^{-3} z_o \Lambda^{1/2}$ is the time delay at the peak of the correlation function. Equation (8) indicates that the peak of the correlation is inversely proportional to the separation of the two line detectors. However, if the separation is too close, the turbulence contamination is severe. In Fig. 6, we have plotted the typical cross-correlation of clear air (no precipitation) for three different separations, 2 cm (top), 1.5 cm (center), and 1 cm (bottom). The left-hand side curves are the temporal correlations induced by turbulence. The turbulence contamination is obvious on all three separations. The right-hand side curves are the subtracted correlations [Eq. (2)]. Most of the turbulence contamination is removed for z_o = 2 cm and z_o = 1.5 cm. For z_o = 1 cm, the left over contamination (peak-to-peak) is over 10%. Therefore, we recommend a vertical separation between 1.5 cm and 2 cm. For most of our measurements, we used 1.5 cm.

4. PRECIPITATION IDENTIFICATION

Our initial objective was to determine how reliably our instrument could detect precipitation. Six channels of signals were used for this purpose, i.e.,

1. $\log \sigma_{1k}$ (2 V/decade),
2. $\log (\sigma_{1k}/\sigma_o)$ (2 V/decade),
3. $\log (\sigma_{2k}/\sigma_o)$ (2 V/decade),
4. $\log (\sigma_{2k}/\sigma_{1k})$ (2 V/decade),
5. peak correlation of C_s (0.7 V/10%), and
6. $\int d\tau\, C_s(\tau)$.

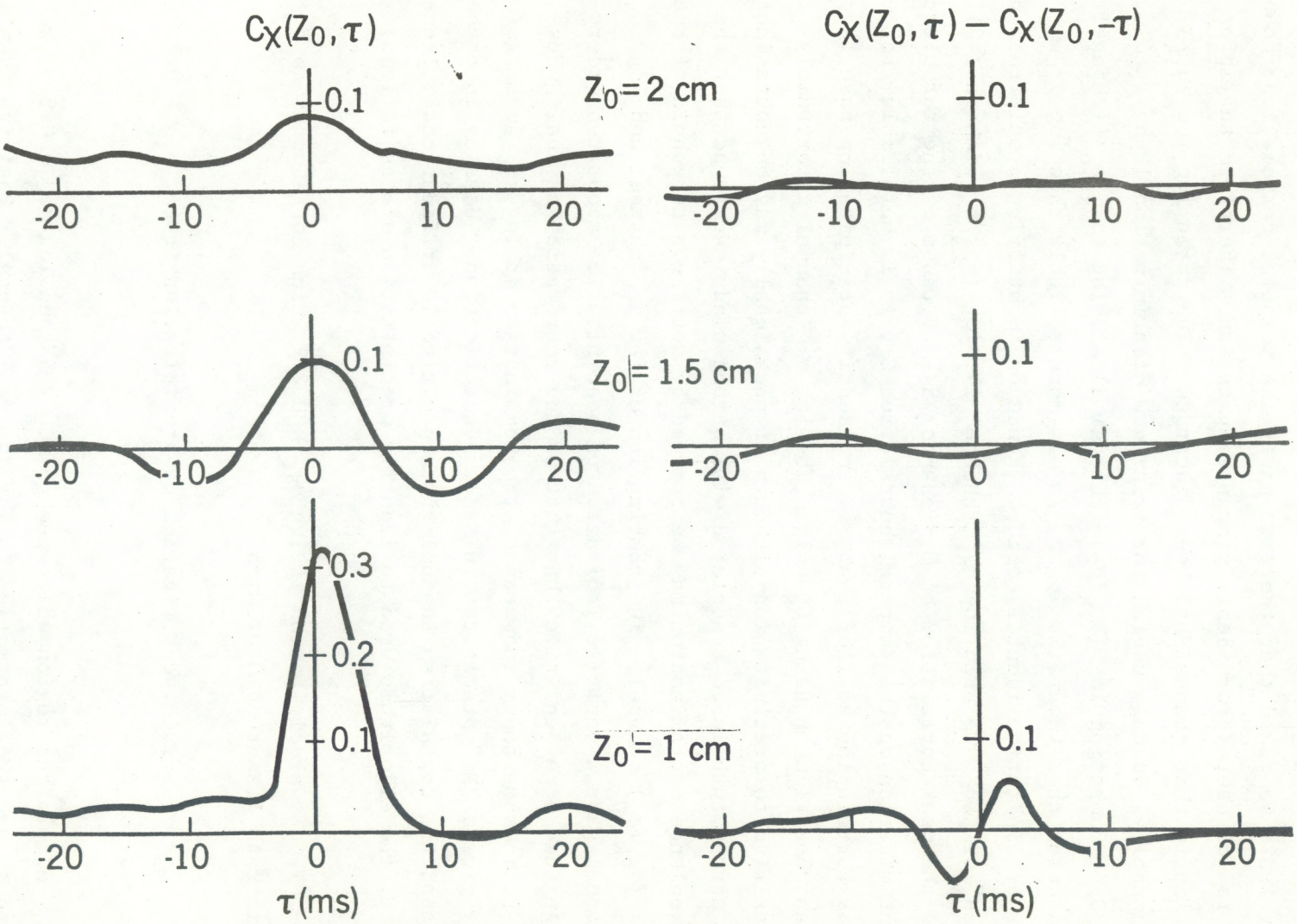

Fig. 6. Cross-correlation of clear air for three different vertical separations Z_o (left-hand side curves). The right-hand side curves are the subtracted correlations of the three separations respectively.

Sample measurements are shown in Figs. 7a and 7b. After examining more than 100 hours of precipitation data collected at Boulder during March 1981 to May 1982, we found that the area under the temporal correlation (channel 6) is not useful for identifying precipitation. Therefore the information in that channel has been discarded. The ratio log $(\sigma_{2k}/\sigma_{1k})$ (channel 4) is only useful for rain/snow discrimination (Wang et al., 1980). Comparing log (σ_{1k}/σ_o) (channel 2) and log (σ_{2k}/σ_o) (channel 3) indicates that the ratio log σ_{2k}/σ_o is more reliable than log σ_{1k}/σ_o for precipitation identification. Hence on identifying precipitation "Yes" or "No", we used log σ_{1k} (channel 1), log (σ_{2k}/σ_o) (channel 3) and the peak correlation of C_s (channel 5). Because of the turbulence contamination on the temporal correlation C_s, it is unreliable, for peak correlation smaller than 5%, to identify precipitation rate less than about 1 mm/h using C_s only. The log σ_{1k} channel is extremely sensitive to precipitation although it occasionally may be contaminated by strong turbulence associated with strong wind. We found that the turbulence contamination may be removed by setting a threshold of the log (σ_{2k}/σ_o) channel. The combination of log σ_{1k} channel and log (σ_{2k}/σ_o) channel gave a positive indication of precipitation about two orders-of-magnitude more sensitive than that of the correlation channel. However, in some heavy snow cases, the combination of log σ_{1k} and log (σ_{2k}/σ_o) may give a "No" precipitation false identification. Usually in these cases, the correlation channel gives positive identifications. Therefore, the algorithms used to identify precipitation are as follows:

1. No precipitation if log $\sigma_{1k} < 0.2$ V which corresponds to a rain rate less than 0.01 mm/h.

2. Positive identification of precipitation if log $\sigma_{1k} > 0.2$ V and peak of $C_s > 5\%$.

3. In the region where peak of $C_s < 5\%$ and log $\sigma_{1k} > 0.2$ V, we need to use the information in log (σ_{2k}/σ_o) channel. Positive identification of precipitation if log $(\sigma_{2k}/\sigma_o) > -1.3$ V, and negative otherwise.

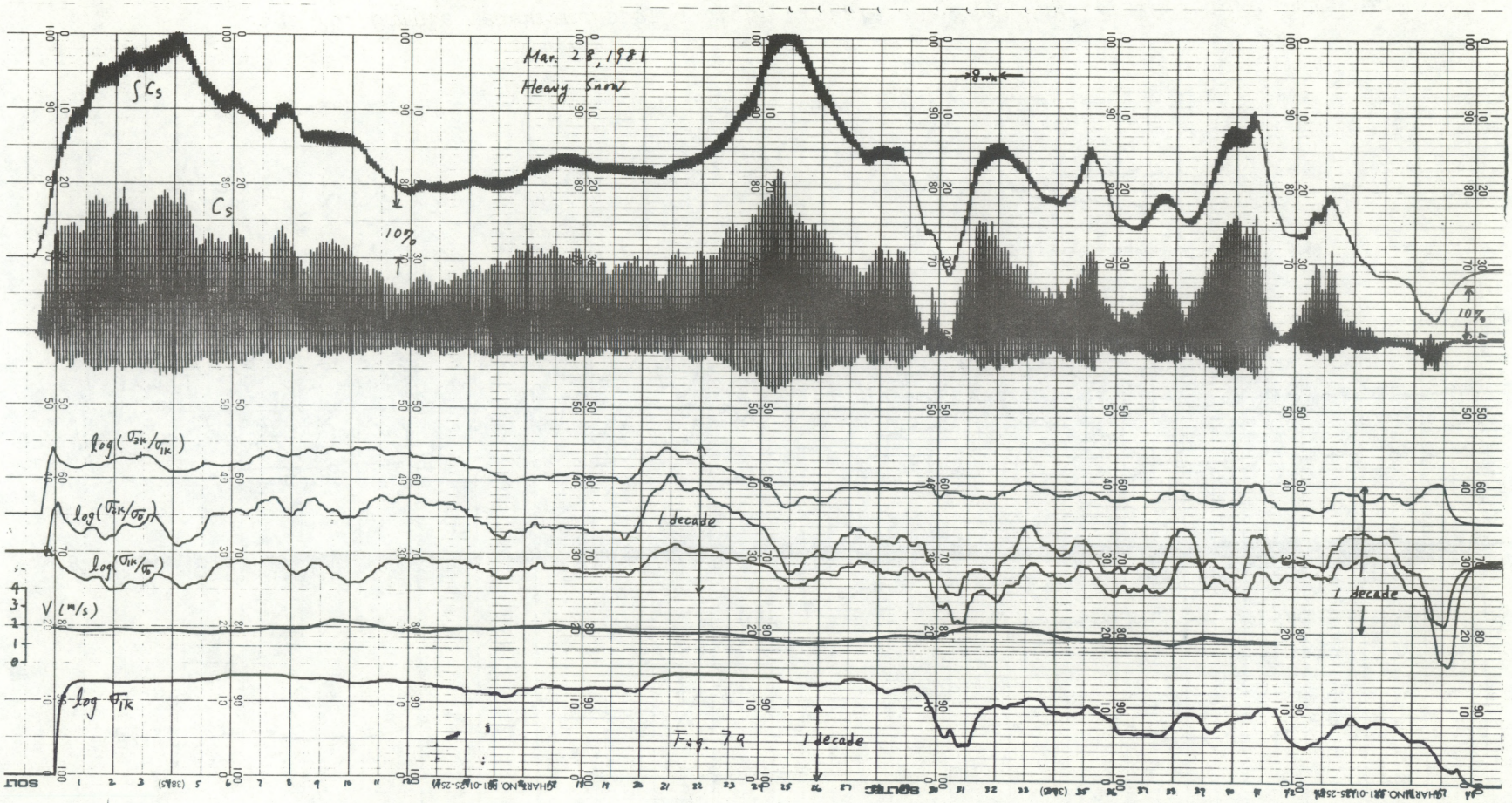

Fig. 7a. Sample measurement of a heavy snow event on March 28, 1981 (see text for details).

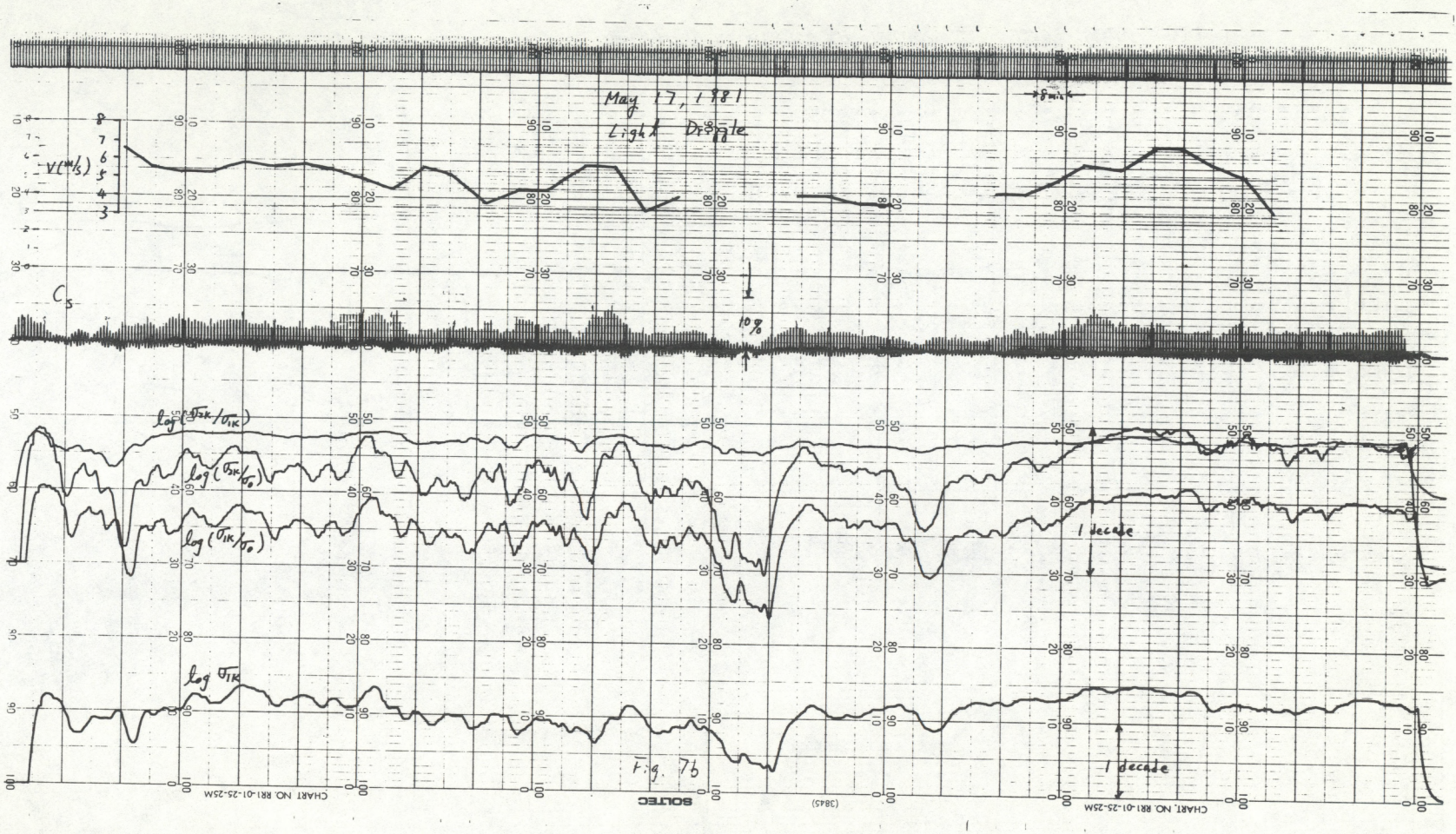

Fig. 7b. Sample measurement of a light drizzle event on May 17, 1981 (see text for details).

A summary of the algorithm is shown in Fig. 8. Using this algorithm table, we found that we usually were able to positively identify rain rate on the order of 0.02 mm/h.

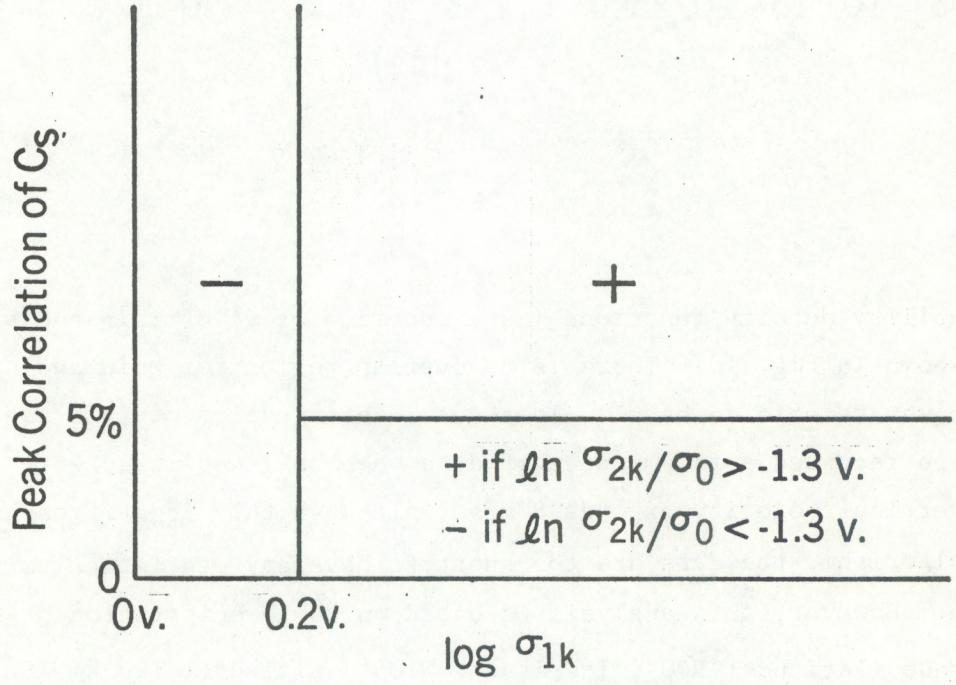

Fig. 8. A summary of the algorithm to identify precipitation.

5. SNOW, RAIN, AND HAIL DISCRIMINATION

Our ultimate objective was to determine different types of precipitation, e.g., snow, rain, and hail. When the peak correlation of C_s exceeds 5%, a reliable vertical velocity (v) of the peak correlation can be obtained. Typical temporal correlations are shown in Fig. 9. The identifications of snow, rain, and hail are as follows:

1. Snow if $v < 3$ m/s,
2. Rain if 3 m/s $< v < 8$ m/s, and
3. Hail (usually mixed with rain) if $v > 8$ m/s.

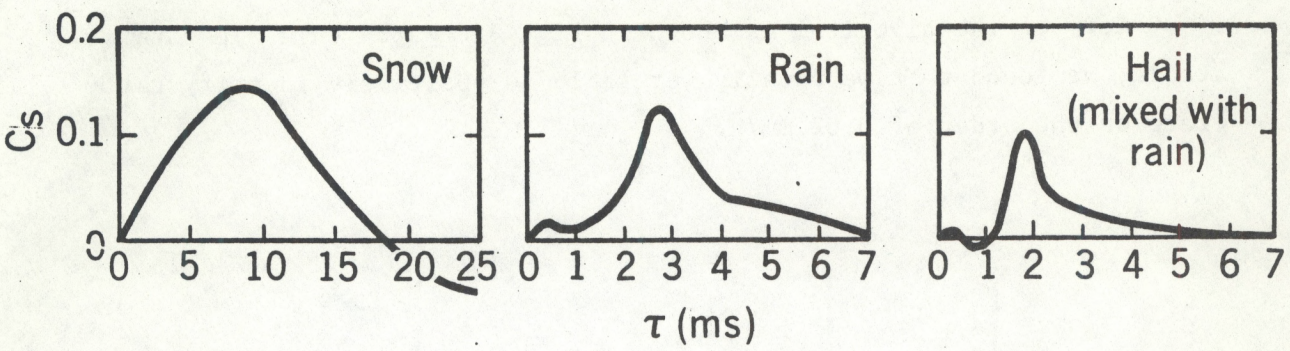

Fig. 9. Typical temporal cross-correlations for snow, rain, and hail.

Probability density functions (as a function of v) of rain and snow are shown in Fig. 10. There is no overlap region for rain and snow. Hence we are able to have a clear-cut identification of rain and snow. We also recorded a few minutes of data when hail was mixed with rain. The vertical velocity exceeds 8 m/s. Although this identifies hail with our algorithm, the data are too short to have any statistical significance. However, this analysis is based on the precipitation at Boulder, Colorado (latitude: N40°, longitude: W105°, altitude: 1.6 km ASL). At different locations, the verticle velocity characteristics may be different.

When the peak correlation of C_s is less than 5% no reliable vertical velocity could be obtained. We used the ratio of σ_{2k}/σ_{1k} to discriminate rain and snow (for details, see Wang et al., 1980). Probability density functions of rain and snow are shown in Fig. 11. The identifications of snow, and rain or hail are as follows:

1. Snow if $\log \sigma_{2k}/\sigma_{1k} < -0.55$, and
2. Rain or hail if $\log \sigma_{2k}/\sigma_{1k} > -0.55$.

The separation between rain and snow is not as good as the case of vertical velocity. A 30% overlap presents some ambiguity of identification, and there is no way to discriminate rain and hail using ratios only.

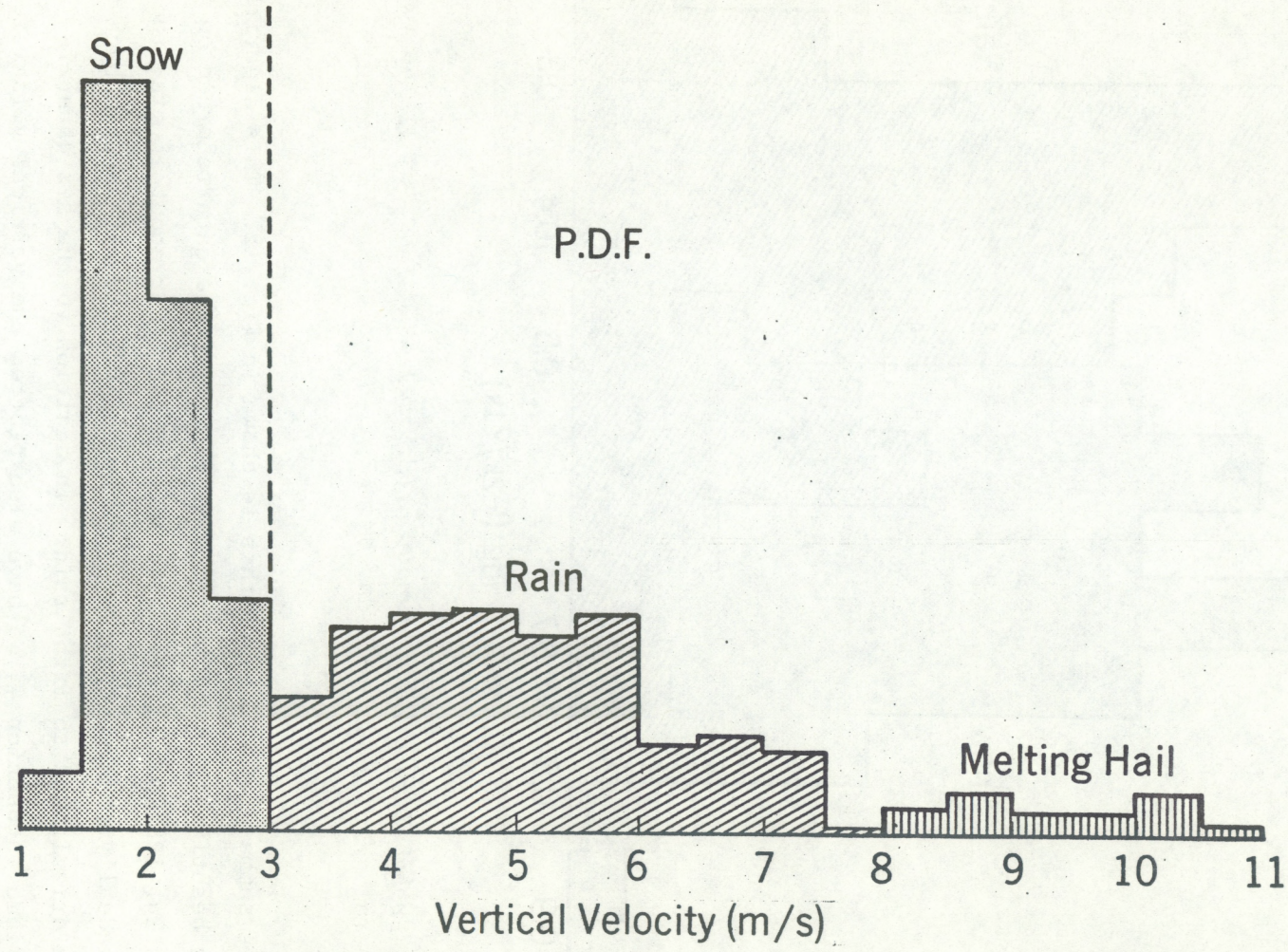

Fig. 10. Probability density functions (P.D.F.) as a function of vertical velocity of rain and snow.

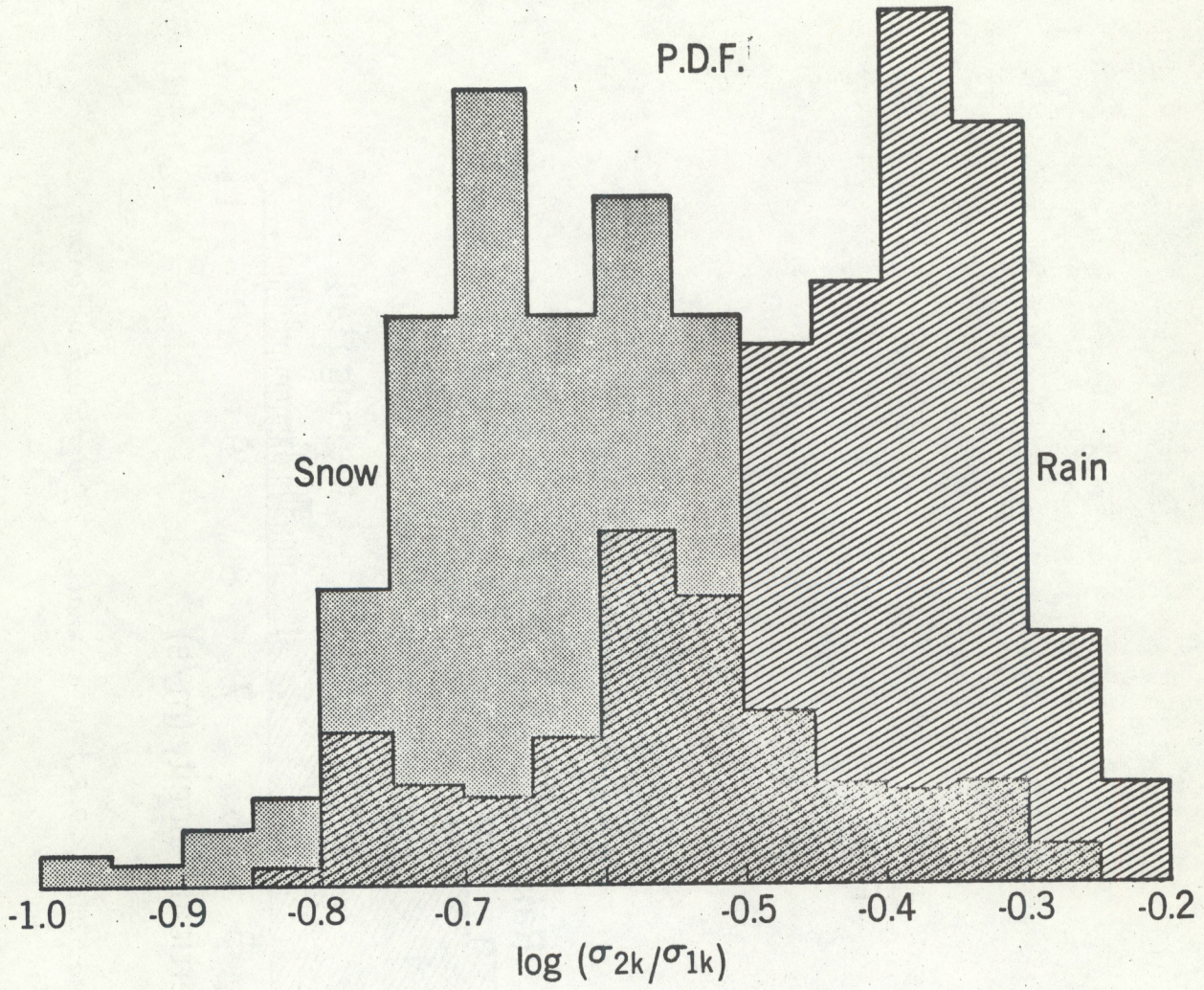

Fig. 11. Probability density function (P.D.F.) as a function of the ratio log (σ_{2K} / σ_{1K}) of rain and snow.

A summary of the algorithms is shown in Fig. 12. This algorithm works beautifully as illustrated in Fig. 13. The data recorded on March 24, 1981 was started with light drizzle for about 15 min, then it gradually changed to snow. At the end of snow, it changed back to light drizzle and to light rain. In addition to the six channels described in Section 4, we have also plotted the vertical velocities obtained from temporal correlations in Fig. 13. The ground observer's report has also been included. In the beginning, the vertical velocity is greater than 3 m/s and log (σ_{2k}/σ_{1k}) is larger than -0.55 (correspond-

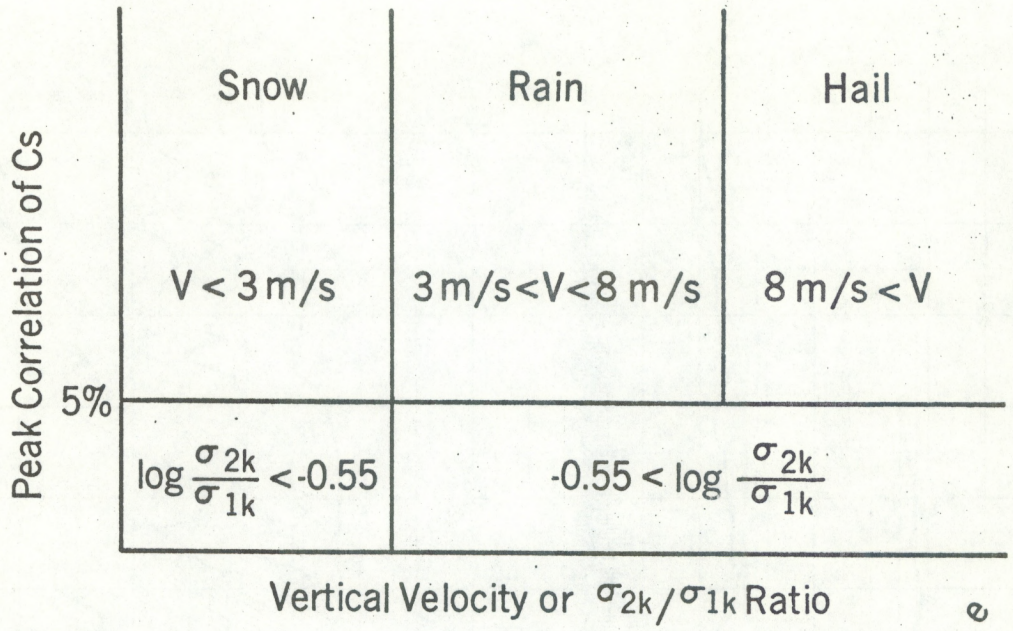

Fig. 12. A summary of the algorithm to discriminate snow, rain, and hail.

ing to 0.4 V, 4 small divisions on the chart) when light drizzle was falling. The velocity then gradually decreased to less than 3 m/s and log (σ_{2k}/σ_{1k}) also decreased to less than 0.4 V when snow started. At the end of snow, when light drizzle took place, the velocity increased to more than 3 m/s and the ratio log (σ_{2k}/σ_{1k}) also increased to above 0.4 V.

Figure 13 also indicates that the frequency channels are more sensitive than the correlation channels for identifying precipitation. In the first 20 min of data, the frequency channels (combinations of log σ_{1k} channel and log (σ_{2k}/σ_o) channel) indicated a positive identification of precipitation while the correlation channel was unable to give a reliable identification. Throughout the 6-h period, the identification of precipitation was positive which agreed with the ground observations. By inspecting more than 100 h of precipitation data, we found that with this algorithm, we are able to positively identify precipitation for a rate as low as 0.02 mm/h.

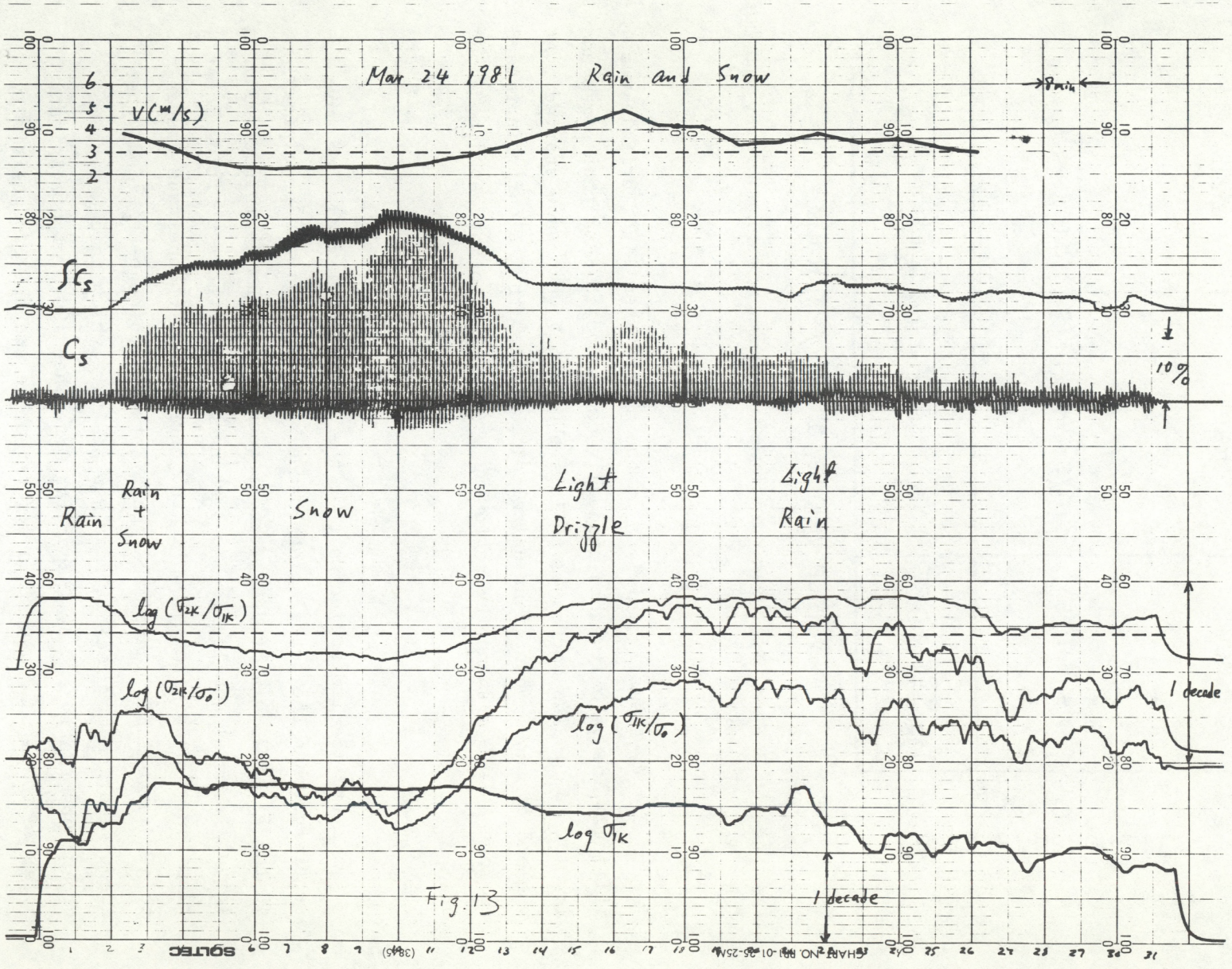

Fig. 13. Sample measurement of an event including rain and snow on March 24, 1981 (see text for details).

Figure 14 indicates a mixture of hail and rain in the beginning of the June 26, 1981 data. The velocity channel indicates the fall velocities exceeding 8 m/s up to 10 m/s, which falls into our algorithm for hail identification. After the first few minutes, hail turned into large rain drops for another 30 min. The vertical velocity exceeded 8 m/s even for rain drops. However, we believe that only rain drops caused by melting hail could reach that velocity. Raising the velocity for hail identification to more than 8 m/s would eliminate this ambiguity but it will also increase the chance of detecting small hail. Unfortunately we do not have enough data to have a more sophisticated analysis.

We have also tried to identify the mixture of rain and snow. One method is to put a buffer zone between rain and snow in the vertical velocity analysis (e.g., between 2.5 m/s and 3.5 m/s) as the region for the mixture. We found that this buffer zone sacrificed the positive identification of pure rain or pure snow with a fall velocity in that region. The other method is to fit the correlation with a known shape of the size distribution (e.g., an exponential distribution). Any significant deviations from the fit (e.g., bimodal distribution) may indicate a mixture of rain and snow. However, we found that the variation of the size distribution of rain (especially for light drizzle) is too uncertain for this method to be practical. Further investigations may be needed on identifying the mixture.

6. DISCUSSIONS

The laser weather identifier identifies precipitation very effectively. Most of the time, we are able to positively identify precipitation with just a few scattered rain drops or snow flakes for a rate on the order of 0.02 mm/h. The system operates with almost no ambiguity to separate rain and snow using vertical velocity if the peak correlation is larger than 5% (equivalent to a rain rate on the order of

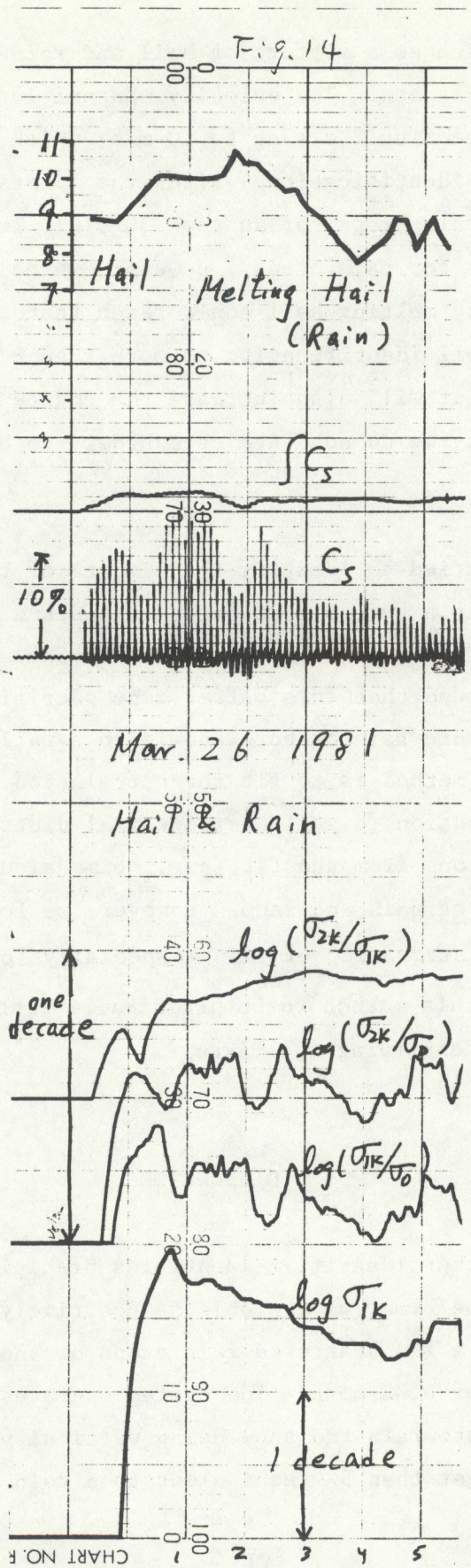

Fig. 14. Sample measurement of a mixture of hail and rain on June 26, 1981 (see text for details).

1 mm/h). For lighter precipitation, rain and snow could be separated using the ratio σ_{2k}/σ_{1k}, though this method may have a 30% ambiguity. With the help of ground temperature measurements, the ambiguity could be lowered. For hail identification, we just do not have enough data to give a result with statistical significance. More hail data should be collected for modifying the algorithms for future systems. Also, all the algorithms were developed on data collected at Boulder, Colorado. For different locations, the statistics of precipitation may not be the same. Further investigations should be carried out at different geographic locations with various types of weather.

At the present time, the data were analyzed manually. However, once the algorithms are fixed, it is straightforward to put the data into a computer for data processing. If rain is positively identified, the path averaged drop size distributions and rain rates could also be obtained (Wang et al., 1979).

Only minor maintenance of the system is required including occasionally realignments and cleaning (probably once a month). The He-Ne laser used as the coherent source has been continuously operated for more than two years, and it is still in good working condition. The receiver electronics has not failed in more than one year of operation.

Acknowledgment -- This work was partially supported by the National Weather Service. The authors are indebted to Dr. Don Acheson, Equipment Development Laboratory, National Weather Service, Silver Springs, Maryland, for his support and valuable discussions.

REFERENCES

Earnshaw, K.B., Ting-i Wang, R.S. Lawrence, and R.G. Greunke, 1978: A feasibility study of identifying weather by laser forward scattering, J. Appl. Meteorol., 17, 1476-1481.

Ochs, G.R., W.D. Cartwright, B.W. Guderian and S.Y. Simpson, 1981: A general purpose correlator, NOAA Tech. Memo. ERL WPL-74.

Wang, Ting-i, and S.F. Clifford, 1975: Use of rainfall-induced optical scintillations to measure path-averaged rain parameters, J. Opt. Soc. Amer., 65, 927-937.

Wang, Ting-i, G. Lerfald, R.S. Lawrence and S.F. Clifford, 1977: Measurement of rain parameters by optical scintillation, Appl. Opt., 16, 2236-2241.

Wang, Ting-i, and R.S. Lawrence, 1977: Measurement of rain parameters by optical scintillation: computer simulation of the correlation method, Appl. Opt., 16, 3176-3179.

Wang, Ting-i, K.B. Earnshaw, and R.S. Lawrence, 1978: Simplified optical path-averaged rain gauge, Appl. Opt., 17, 384-390.

Wang, Ting-i, K.B. Earnshaw, and R.S. Lawrence, 1979: Path-averaged measurements of rain rate and raindrop size distribution using a fast-response optical sensor, J. Appl. Meteorol., 18, 654-660.

Wang, Ting-i, R. Lataitis, K.B. Earnshaw, and E. Moroz, 1980: Analysis of data from two laser weather identifier systems, NOAA Tech. Memo. ERL WPL-65.

Wang, Ting-i, G.R. Ochs, W.D. Cartwright, B.W. Guderian, and S.Y. Simpson, 1982: A prototype laser weather identifier, NOAA Tech. Memo. ERL WPL-95.

Wang, Ting-i, R. Lataitis, R.S. Lawrence, and G.R. Ochs, 1982: Laser weather identifier: present and future, Accepted by J. Appl. Meteorol.